Protocol of a quantum walk in circuit QED

Jia-Qi Zhou, Ling Cai, Qi-Ping Su,* and Chui-Ping Yang
Department of Physics, Hangzhou Normal University, Hangzhou, Zhejiang 311121, China

(Received 17 February 2019; published 25 July 2019)

Implementation of a discrete-time quantum walk (DTQW) with superconducting qubits is difficult since on-chip superconducting qubits cannot hop between lattice sites. We propose an efficient protocol for the implementation of DTQW in circuit quantum electrodynamics (QED), in which only $N+1$ qutrits, N cavities, and other assistant devices are needed for an N-step DTQW. The operation of each DTQW step is very quick because only resonant processes are adopted. The numerical simulations show that high-similarity DTQW with a number of steps up to 20 is feasible with present-day circuit QED techniques. This protocol can help to study properties and applications of many-step DTQW in experiments, and can be extended to implement multidimensional DTQW in circuit QED or other quantum systems.

DOI: 10.1103/PhysRevA.100.012343

I. INTRODUCTION

Circuit quantum electrodynamics (QED), composed of superconducting qubits and microwave resonators or cavities, has attracted substantial attention because of its controllability, integrability, ready fabrication, and potential scalability [1–11] in quantum information and quantum computation. Strong coupling and ultrastrong coupling of a qubit with a microwave cavity in experiments have been reported [1,12]. The level spacings of superconducting qubits can be rapidly adjusted ($1 \sim 3$ ns) [13–16], and their coherence time is improved rapidly [13,17–21]. The circuit QED is considered as one of the most feasible candidates for quantum computation and quantum simulation [10,11].

The quantum walk is the extension of the classical random walk, which has wide applications in quantum algorithms [22–24], quantum simulation [25–28], universal quantum computation [29–31], and so on [32,33]. In the standard discrete-time quantum walk (DTQW), there is a walker moving with respect to the state of a coin. The evolutions of the walker and the coin are characterized by a unitary operator $U = WC$. In each step of a 1-dimensional (1D) DTQW, at first, the coin with states $|0\rangle_c$ and $|1\rangle_c$ is tossed by the operator,

$$C = \cos\theta|0\rangle_c\langle 0| + \sin\theta|0\rangle_c\langle 1| + \sin\theta|1\rangle_c\langle 0| - \cos\theta|1\rangle_c\langle 1|, \quad (1)$$

with $\theta \in (0, \pi/2)$, and then the walker is shifted by

$$W = \sum_j |j\rangle\langle j| \otimes |0\rangle_c\langle 0| + |j+1\rangle\langle j| \otimes |1\rangle_c\langle 1|, \quad (2)$$

where the integer j represents sites of the walker in the 1D line. Though this shift operator W is different from that of the standard DTQW, two shift operators are actually equivalent to each other [34,35]. The implementations of DTQW have been achieved in several quantum systems, such as linear optics [24–26,36–38], ion traps [39,40], and neutral atom traps [41].

But it is not easy to implement DTQW in circuit QED. In other quantum systems, the coin and the walker can be encoded with a single qubit, such as single photons or ions, while the encoding of the coin and the walker with a superconducting qubit is difficult, since the superconducting qubits in circuit QED cannot move like photons or ions. There are only a few DTQW schemes in circuit QED. In [42–44], the phase space of superposition states in a cavity is used to encode the walker's position and a coupled qubit is used as the coin. Due to the adopted nonorthogonal states of the cavity and the limitation of the phase space, the generality and the scalability of this type of scheme are inevitable problems. In [45], a 1D DTQW scheme is proposed, in which a pair of superconducting qubits is used as a node and nearest-neighbor qubits are coupled via tunable couplers. The walker moves in the 1D line of nodes and the coin is encoded by the position of the occupied qubit in each node.

In recent years, quantum information processing with qudits (d-level systems), including qutrits (i.e., $d = 3$), has been attracting increasing interest, since qudits (with $d > 2$) can be used to encode more information. For example, quantum information processing and tomography of nanoscale semiconductor devices were studied [46,47]. In [48], quantum state transfer on a one-dimensional lattice of superconducting qutrits was studied. In [49,50], efficient schemes for quantum state transfer of a qutrit in circuit QED were proposed.

In this paper, we propose an efficient and simple protocol for implementation of DTQW in circuit QED, in which only $N+1$ qutrits (with 3 energy levels, tunable), N cavities (i.e., the couplers), and assistant devices (such as microwave lines for classical pulses and readout devices) are needed for an N-step DTQW. Since only resonant processes are adopted, the operation of each DTQW step is very quick. With this protocol, arbitrary initial states of the coin can be prepared and arbitrary operation of the coin can be implemented easily. To estimate the implementation of this protocol and the effects of parameters, we numerically simulate the DTQW in a superconducting system with the number of steps up to 20. It indicates that this protocol is feasible with the present circuit

*sqp@hznu.edu.cn

QED technology and can be used to implement a many-step DTQW. Because of the scalability and rapid improvement of circuit QED technology, this protocol can help to study properties and applications of many-step DTQW in experiments, which is important for the development of quantum information science.

II. A 1D DTQW protocol

As shown in Fig. 1, the setup consists of $N+1$ tunable flux qutrits (with energy levels $|g\rangle$, $|e\rangle$, and $|f\rangle$) and N cavities (e.g., 1D transmission line resonators, which can couple with qutrits via capacitors). Suppose all qutrits have the same energy levels (only at one bias point) and the frequency of cavities (ω_c) is equal to the $|g\rangle \leftrightarrow |e\rangle$ transition frequency of the qutrits (i.e., the identical ω_{eg} at the bias point). The walker's position is represented by the position of the qutrit in a nonground state (i.e., superposition state of $|e\rangle$ and $|f\rangle$), and the coin states $|0\rangle_c$ and $|1\rangle_c$ are represented by the states $|f\rangle$ and $|e\rangle$, respectively. In this case, an arbitrary initial state of the coin can be prepared easily by applying corresponding pulses to the qutrits. Suppose all cavities are initially in the ground state $|0\rangle$ and decoupled with qutrits; the steps for the implementation of the DTQW are as follows.

Step I: Tossing the coin by applying a pulse (with the Rabi frequency Ω) to each qutrit. The frequency, duration, and initial phase of the pulses are ω_{fe}, t_I, ϕ, respectively. In the interaction picture, the Hamiltonian for qutrits interacting with the pulses is

$$H_{I,1} = \sum_j \Omega(e^{i\phi}|e\rangle_j\langle f| + e^{-i\phi}|f\rangle_j\langle e|).$$

This Hamiltonian makes the following transformations for states of qutrit j ($j = 1, 2, 3, \dots, N+1$):

$$\begin{aligned} |g\rangle_j &\to |g\rangle_j, \\ |e\rangle_j &\to \cos(\Omega t_I)|e\rangle_j - ie^{-i\phi}\sin(\Omega t_I)|f\rangle_j, \\ |f\rangle_j &\to -ie^{i\phi}\sin(\Omega t_I)|e\rangle_j + \cos(\Omega t_I)|f\rangle_j. \end{aligned} \tag{3}$$

This shows that an arbitrary unitary operator of the coin can be achieved by applying suitable pulses. If we set $t_I = \theta/\Omega$ and $\phi = -\pi/2$, this operation of the coin is just that of $\sigma_z C$, where C is the coin operator in Eq. (1) and $\sigma_z = |0\rangle_c\langle 0| - |1\rangle_c\langle 1|$. The shift operation of the walker with respect to the coin state will be accomplished by the following two steps.

Step II: Adjusting the level spacing of qutrit j to couple it with cavity j (assuming the coupling strength $g_j = g$ with $j = 1, 2, 3, \dots, N$), i.e., $\omega_{eg} = \omega_c$. The Hamiltonian in the interaction picture is

$$H_{I,2} = \sum_j g(a_j|e\rangle_j\langle g| + a_j^+|g\rangle_j\langle e|).$$

After the evolution time $t_{II} = \pi/(2g)$ (i.e., $gt_{II} = \pi/2$), the transformations for the states of the qutrit j and the cavity j are

$$\begin{aligned} |g\rangle_j|0\rangle_j &\to |g\rangle_j|0\rangle_j, \\ |e\rangle_j|0\rangle_j &\to -i|g\rangle_j|1\rangle_j, \\ |f\rangle_j|0\rangle_j &\to |f\rangle_j|0\rangle_j. \end{aligned} \tag{4}$$

Step III: Adjusting the level spacings of qutrits j and $j+1$ to decouple the qutrit j from cavity j while coupling the qutrit $j+1$ with cavity j (assuming the coupling strength $g'_j = \mu$ with $j = 1, 2, 3, \dots, N$). Now the Hamiltonian in the interaction picture becomes

$$H_{I,3} = \sum_j \mu(a_j|e\rangle_{j+1}\langle g| + a_j^+|g\rangle_{j+1}\langle e|).$$

After the evolution time $t_{III} = \pi/(2\mu)$, the transformations for the states of the cavity j and the qutrit $j+1$ are

$$\begin{aligned} |0\rangle_j|g\rangle_{j+1} &\to |0\rangle_j|g\rangle_{j+1}, \\ |1\rangle_j|g\rangle_{j+1} &\to -i|0\rangle_j|e\rangle_{j+1}. \end{aligned} \tag{5}$$

Finally, the level spacing of qutrit $j+1$ is adjusted to decouple it from cavity j.

If the walker is initially in position j (i.e., the qutrit j is excited), after step II and step III, it will move into position $j+1$ (i.e., the qutrit $j+1$) with the coin state $|1\rangle_c$ ($|e\rangle_{j+1}$) or it will stay in position j (i.e., the qutrit j) with the coin state $|0\rangle_c$ ($|f\rangle_j$). This shift operation of the walker achieved in steps II and III can be expressed as $W\sigma_z$.

Now the standard DTQW operation $U = WC$ is achieved with the operational time $t = t_I + t_{II} + t_{III}$. In Fig. 2, the evolutions of the states of the qutrits j, $j+1$ and the cavity j with steps I, II, and III are demonstrated by assuming an initial state of $|j\rangle|1\rangle_c$ (i.e., $|e\rangle_j$). Repeating steps I, II, and III N times, an N-step 1D DTQW is realized.

III. POSSIBLE EXPERIMENTAL IMPLEMENTATION

In this section, we discuss the feasibility of the implementation of this DTQW protocol with DTQW steps up to 20 by numerical simulations. In all simulations, we set $\theta = \pi/4$ for the coin operator and assume that the walker starts from the qutrit 1. By considering dissipation and dephasing, the

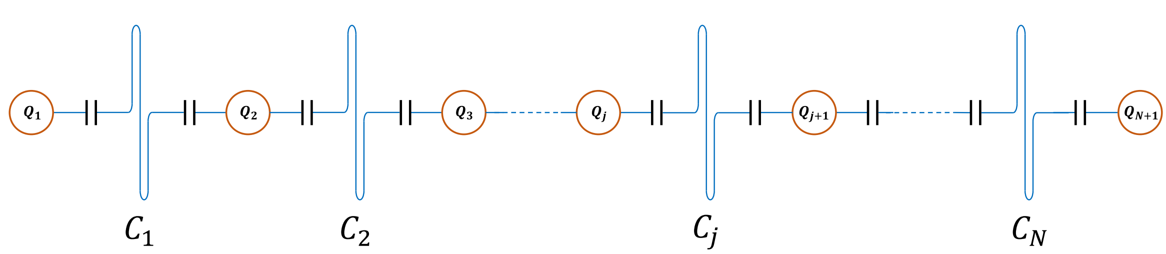

FIG. 1. Setup for implementation of DTQW in circuit QED, which mainly consists of $N+1$ qutrits and N cavities (e.g., 1D transmission line resonators).

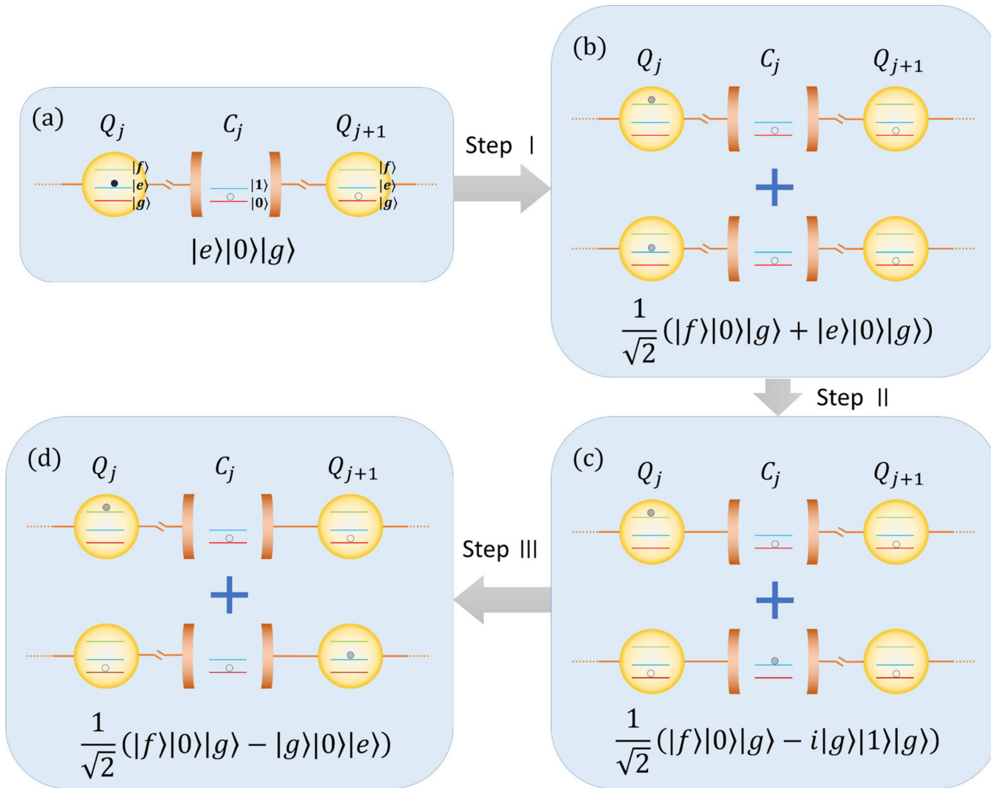

FIG. 2. Illustration of implementing steps of DTQW and state evolutions by assuming that energy level $|e\rangle$ of the qutrit j is initially occupied (i.e., initially the walker is at the position j and the coin state is $|1\rangle$). The small circles indicate the occupied energy levels. Hollow circles represent the occupation of ground states and the shade of solid circles represents the probability of the occupation of nonground states. $\theta = \pi/4$ has been assumed for the coin operator C.

evolving of the system is determined by the master equation

$$\frac{d\rho}{dt} = -i[H_{I,k}, \rho] + \sum_j \kappa_{a_j}\mathcal{L}[a_j] + \sum_j \gamma_{ef,j}\mathcal{L}[\sigma_{ef,j}^-] + \gamma_{gf,j}\mathcal{L}[\sigma_{gf,j}^-] + \gamma_{ge,j}\mathcal{L}[\sigma_{ge,j}^-] + \sum_j \gamma_{e\varphi,j}\mathcal{L}[\sigma_{ee,j}] + \gamma_{f\varphi,j}\mathcal{L}[\sigma_{ff,j}], \quad (6)$$

where $\mathcal{L}[\Lambda] = \Lambda\rho\Lambda^+ - \Lambda^+\Lambda\rho/2 - \rho\Lambda^+\Lambda/2$ (with $\Lambda = a_j, \sigma_{ef,j}^-, \sigma_{gf,j}^-, \sigma_{ge,j}^-, \sigma_{ee,j}, \sigma_{ff,j}$), $\sigma_{ef,j}^- = |e\rangle_j\langle f|$, $\sigma_{gf,j}^- = |g\rangle_j\langle f|$, $\sigma_{ge,j}^- = |g\rangle_j\langle e|$, $\sigma_{ee,j} = |e\rangle_j\langle e|$, and $\sigma_{ff,j} = |f\rangle_j\langle f|$; κ_{a_j} is the decay rate of cavity j; $\gamma_{ef,j}$ ($\gamma_{gf,j}$) is the energy relaxation rate for the level $|f\rangle$ associated with the decay path $|f\rangle \to |e\rangle$ ($|f\rangle \to |g\rangle$) of qutrit j; $\gamma_{ge,j}$ is the energy relaxation rate of the level $|e\rangle$; and $\gamma_{f\varphi,j}$ ($\gamma_{e\varphi,j}$) is the dephasing rate of the level $|f\rangle$ ($|e\rangle$) of qutrit j. In the simulations, we will divide each DTQW step into six processes: One process for the classical pulse (with $H_{I,1}$), two resonant processes (with $H_{I,2}$ and $H_{I,3}$), and three level spacing adjusting processes, as shown in Sec. II. Each process is calculated by the master equation, and the density matrix obtained from previous process is used as the initial density matrix of the next process. Since the three level spacing adjusting processes are very rapid, we set each adjusting time as 2 ns and set the corresponding Hamiltonian $H_I = 0$ for simplicity.

In DTQW experiments, the probability distribution $P(j)$ of the walker is always easy to measure. So we calculate the similarity $S = [\sum_j \sqrt{P_{me}(j)P_{id}(j)}]^2$, which is a generalization of the classical fidelity between two distributions and has been widely used in DTQW experiments [25,27], to compare the $P_{me}(j)$ from result density matrix of the master Eq. (6) with the ideal $P_{id}(j)$ of the standard DTQW. In numerical simulations, flux qutrits are adopted and the decoherence parameters used are (i) $\gamma_{e\varphi,j}^{-1} = 2.5$ μs, $\gamma_{f\varphi,j}^{-1} = 2.5$ μs; (ii) $\gamma_{ge,j}^{-1} = 5$ μs, $\gamma_{ef,j}^{-1} = 2.5$ μs, $\gamma_{gf,j}^{-1} = 7.5$ μs; and (iii) $\kappa_{a_j}^{-1} = 10$ μs [51,52]. Note that decoherence time ranging from 40 μs to 1 ms has been reported for a flux qudit [21,53–56]. These values of decoherence parameters for flux qutrits have considered the possible reduction of the coherence time away from the flux-bias sweet spot, the Purcell effect, etc. We denote this set of the decoherence parameters as T and the above choice of T as T_0. For simplicity, we will set the coupling strengths $g_j = g_j' = g$. We will study the effects of the coupling strength g, Rabi frequency Ω, initial state of the coin $|\phi_{c0}\rangle$, number of DTQW steps N, and decoherence time set T on the similarity S.

In Fig. 3(a), the similarity versus $g/2\pi$ is plotted respectively for $|\phi_{c0}\rangle = |0\rangle_c$, $|1\rangle_c$, and $(|0\rangle_c + i|1\rangle_c)/\sqrt{2}$ [i.e., $|f\rangle$, $|e\rangle$, and $(|f\rangle + i|e\rangle)/\sqrt{2}$], with $N = 10$ and $\Omega/2\pi = 100$ MHz [57]. It is shown that different initial states of the coin lead to different similarities. Since each initial state of the coin is a superposition of $|0\rangle_c$ and $|1\rangle_c$ (i.e., $|f\rangle$ and $|e\rangle$), the lowest similarity for all initial states should be that with the initial state $|0\rangle_c$ (i.e., $|f\rangle$). This phenomenon is

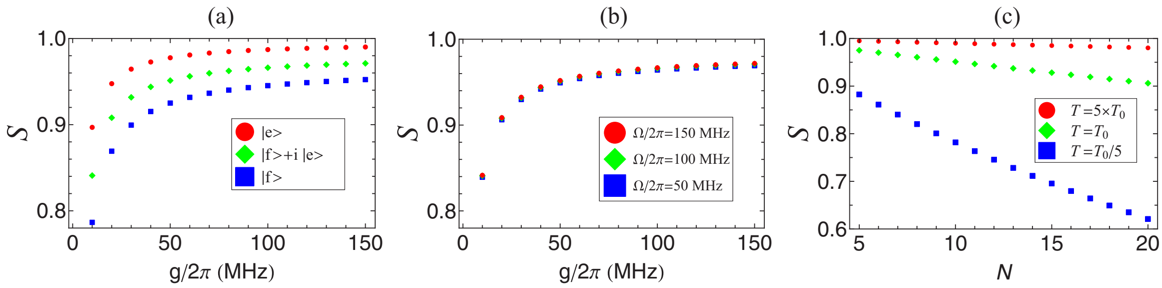

FIG. 3. Similarity versus $g/2\pi$ is plotted respectively (a) for initial states of the coin $|0\rangle_c$, $|1\rangle_c$, $(|0\rangle_c + i|1\rangle_c)/\sqrt{2}$ [i.e., $|f\rangle$, $|e\rangle$, and $(|f\rangle + i|e\rangle)/\sqrt{2}$], with $N = 10$ and $\Omega/2\pi = 100$ MHz; (b) for $\Omega/2\pi = 50, 100, 150$ MHz, with $N = 10$ and the initial state of the coin $(|0\rangle_c + i|1\rangle_c)/\sqrt{2}$. (c) Similarity versus number of steps N is plotted respectively for $T = 5T_0, T_0, T_0/5$, with $g/2\pi = 50$ MHz, $\Omega/2\pi = 100$ MHz, and the initial state of the coin $(|0\rangle_c + i|1\rangle_c)/\sqrt{2}$.

mainly due to two facts: (1) the probability that the walker stays on $|f\rangle$ is larger if the walker starts from $|f\rangle$, which has been confirmed numerically for $N \leqslant 20$; (2) the lifetime of $|f\rangle$ is shorter than that of $|e\rangle$ for all qutrits. As $g/2\pi = 50$ MHz, this shows that the similarity S is larger than 0.925 for an arbitrary initial state of the coin in the 10-step DTQW. Moreover, the similarity increases with the increasing of g as expected. It is shown that high similarity of this protocol can be achieved with the present technology of circuit QED.

In Fig. 3(b), similarity versus $g/2\pi$ is plotted respectively for $\Omega/2\pi = 50, 100, 150$ MHz, with $N = 10$ and $|\phi_{c0}\rangle = (|0\rangle_c + i|1\rangle_c)/\sqrt{2}$. This shows that the similarity is not sensitive to the Rabi frequency Ω.

In Fig. 3(c), similarity versus number of step N is plotted respectively for $T = 5T_0, T_0, T_0/5$, with $g/2\pi = 50$ MHz, $\Omega/2\pi = 100$ MHz, and $|\phi_{c0}\rangle = (|0\rangle_c + i|1\rangle_c)/\sqrt{2}$. This indicates that similarity decreases with the increasing of N and with the decreasing of T as expected. For larger T, similarity decreases more slowly with the increasing of the step N. For larger N, similarity is more sensitive to the variance of T. For $N = 20$, we obtain similarity $S \sim 0.980, 0.906, 0.621$ with $T = 5T_0, T_0, T_0/5$, respectively. If the coherence times of the devices are not very small, high similarity for a many-step DTQW can be achieved with this DTQW protocol in circuit QED.

In actual experiments, there are always some imperfections of devices and operations which lead to errors of final states. Here we estimate the effects of three possible error sources on the similarity independently. In the following calculations, we set $g/2\pi = 50$ MHz, $\Omega/2\pi = 100$ MHz, $N = 10$, and the initial state of the coin $(|0\rangle_c + i|1\rangle_c)/\sqrt{2}$. The first error source we considered is that the condition $gt_i = \pi/2$ may not be satisfied in the two resonant processes due to the error of the coupling strength g or the operational time t_i. In Fig. 4(a), the similarity versus $R_g = \bar{g}/g$ is plotted, where $\bar{g}$ is the actual coupling strength used rather than the perfect g in theory. Note that the effect of the error of operational time t_i on the similarity is the same as that of error of g. This shows that the similarity $\gtrsim$0.9 can be maintained with the error of g within 5%. In Fig. 4(b), the similarity versus $\delta = \omega_c - \omega_{eg}$ is plotted, which estimates effects of the imperfect adjusting of qutrit levels. This shows that the similarity $\gtrsim$0.86 can be maintained with the error of $\delta/2\pi$ within 10 MHz. In Fig. 4(c), the similarity versus $\Delta = \omega_{fe} - \omega_{eg}$ is plotted, which estimates effects of the unwanted couplings of cavities and the unwanted interaction of pulses with the $|e\rangle \leftrightarrow |f\rangle$ transition of qutrits. In this case, we replaced the $H_{I,k}$ $(k = 1, 2, 3)$ used in the master equation with $\tilde{H}_{I,k}$:

$$\tilde{H}_{I,1} = H_{I,1} + \sum_j \Omega(-ie^{i\Delta t}|g\rangle_j\langle e| + ie^{-i\Delta t}|e\rangle_j\langle g|),$$

$$\tilde{H}_{I,2} = H_{I,2} + \sum_j g(a_j e^{i\Delta t}|f\rangle_j\langle e| + a_j^{+} e^{-i\Delta t}|e\rangle_j\langle f|),$$

$$\tilde{H}_{I,3} = H_{I,3} + \sum_j \mu(a_j e^{i\Delta t}|f\rangle_{j+1}\langle e| + a_j^{+} e^{-i\Delta t}|e\rangle_{j+1}\langle f|).$$

This shows that the similarity $\gtrsim$0.9 can be maintained with $\Delta/2\pi > 1.4$ GHz, which can be achieved easily for flux qutrits.

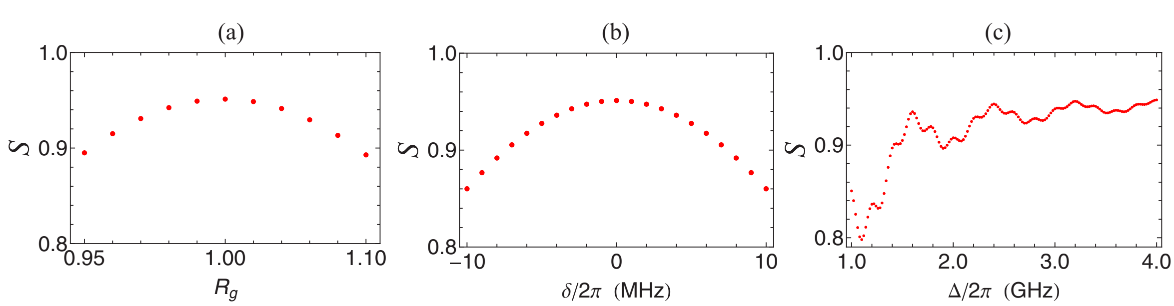

FIG. 4. Similarity versus (a) $R_g = \bar{g}/g$ to estimate the effects of a possible imperfect set of the coupling strength g, (b) $\delta = \omega_c - \omega_{eg}$ to estimate the effects of a possible imperfect adjusting of level spacing of qutrits, and (c) $\Delta = \omega_{fe} - \omega_{eg}$ to estimate the effects of the unwanted coupling of cavities and the unwanted interaction of pulses with the $|e\rangle \leftrightarrow |f\rangle$ transition of qutrits.

IV. CONCLUSIONS

We have presented a protocol for implementing standard DTQW in circuit QED. The protocol is simple and efficient; only $N+1$ qutrits, N cavities, and other assistant devices are needed for an N-step DTQW and the operational time for each step is rather short due to the adoption of resonant processes. With this protocol, arbitrary initial states of the coin can be prepared and arbitrary operation of the coin can be implemented easily, which is necessary for general research and applications of DTQW. The numerical simulations prove that high-similarity DTQW with $N \leqslant 20$ is feasible with present-day circuit QED techniques. This DTQW protocol is quite general and can be extended to implement multidimensional DTQW in circuit QED or other quantum systems.

ACKNOWLEDGMENTS

This work was supported in part by the Ministry of Science and Technology of China under Grant No. 2016YFA0301802, the National Natural Science Foundation of China under Grants No. 11504075, No. 11074062, and No. 11374083, and the Key Research and Development Program of Guangdong Province (Grant No. 2018B030326001).

[1] A. Wallraff, D. I. Schuster, A. Blais, L. Frunzio, R. S. Huang, J. Majer, S. Kumar, S. M. Girvin and R. J. Schoelkopf, Circuit quantum electrodynamics: Coherent coupling of a single photon to a Cooper pair box, Nature (London) **431**, 162 (2004).
[2] M. Mariantoni, H. Wang, R. C. Bialczak, M. Lenander, E. Lucero, M. Neeley, A. D. O'Connell, D. Sank, M. Weides, J. Wenner, T. Yamamoto, Y. Yin, J. Zhao, J. M. Martinis, and A. N. Cleland, Photon shell game in three-resonator circuit quantum electrodynamics, Nat. Phys. **7**, 287 (2011).
[3] X. Gu, A. F. Kockum, A. Miranowicz, Y. X. Liu, and F. Nori, Microwave photonics with superconducting quantum circuits, Phys. Rep. **718–719**, 1 (2017).
[4] A. F. Kockum, A. Miranowicz, S. D. Liberato, S. Savasta, and F. Nori, Ultrastrong coupling between light and matter, Nat. Rev. Phys. **1**, 19 (2019).
[5] C. P. Yang, S. I. Chu, and S. Y. Han, Possible realization of entanglement, logical gates, and quantum-information transfer with superconducting-quantum-interference-device qubits in cavity QED, Phys. Rev. A **67**, 042311 (2003).
[6] J. Q. You and F. Nori, Quantum information processing with superconducting qubits in a microwave field, Phys. Rev. B **68**, 064509 (2003).
[7] A. Blais, R. Huang, A. Wallra, S. Girvin, and R. Schoelkopf, Cavity quantum electrodynamics for superconducting electrical circuits: An architecture for quantum computation, Phys. Rev. A **69**, 062320 (2004).
[8] J. Q. You and F. Nori, Superconducting circuits and quantum information, Phys. Today **58**(11), 42 (2005).
[9] J. Q. You and F. Nori, Atomic physics and quantum optics using superconducting circuits, Nature (London) **474**, 589 (2011).
[10] I. Buluta, S. Ashhab, and F. Nori, Natural and artificial atoms for quantum computation, Rep. Prog. Phys. **74**, 104401 (2011).
[11] Z. L. Xiang, S. Ashhab, J. Q. You, and F. Nori, Hybrid quantum circuits: Superconducting circuits interacting with other quantum systems, Rev. Mod. Phys. **85**, 623 (2013).
[12] T. Niemczyk, F. Deppe, H. Huebl, E. P. Menzel, F. Hocke, M. J. Schwarz, J. J. Garcia-Ripoll, D. Zueco, T. Hummer, E. Solano, A. Marx, and R. Gross, Circuit quantum electrodynamics in the ultrastrong-coupling regime, Nat. Phys. **6**, 772 (2010).
[13] R. Barends, J. Kelly, A. Megrant, D. Sank, E. Jeffrey, Y. Y. Chen, Y. Yin, B. Chiaro, J. Mutus, C. Neill, P. O'Malley, P. Roushan, J. Wenner, T. C. White, A. N. Cleland, and J. M. Martinis, Coherent Josephson Qubit Suitable for Scalable Quantum Integrated Circuits, Phys. Rev. Lett. **111**, 080502 (2013).
[14] M. Neeley, M. Ansmann, R. C. Bialczak, M. Hofheinz, N. Katz, E. Lucero, A. O'Connell, H. Wang, A. N. Cleland, and J. M. Martinis, Process tomography of quantum memory in a Josephson-phase qubit coupled to a two-level state, Nat. Phys. **4**, 523 (2008).
[15] P. J. Leek, S. Filipp, P. Maurer, M. Baur, R. Bianchetti, J. M. Fink, M. Goppl, L. Steffen, and A. Wallraff, Using sideband transitions for two-qubit operations in superconducting circuits, Phys. Rev. B **79**, 180511(R) (2009).
[16] J. D. Strand, M. Ware, F. Beaudoin, T. A. Ohki, B. R. Johnson, A. Blais, and B. L. T. Plourde, First-order sideband transitions with flux-driven asymmetric transmon qubits, Phys. Rev. B **87**, 220505(R) (2013).
[17] J. M. Chow, J. M. Gambetta, A. D. Crcoles, S. T. Merkel, J. A. Smolin, C. Rigetti, S. Poletto, G. A. Keefe, M. B. Rothwell, J. R. Rozen, M. B. Ketchen, and M. Steffen, Universal Quantum Gate Set Approaching Fault-Tolerant Thresholds with Superconducting Qubits, Phys. Rev. Lett. **109**, 060501 (2012).
[18] J. B. Chang, M. R. Vissers, A. D. Corcoles, M. Sandberg, J. Gao, D. W. Abraham, J. M. Chow, J. M. Gambetta, M. B. Rothwell, G. A. Keefe, M. Steffen, and D. P. Pappas, Improved superconducting qubit coherence using titanium nitride, Appl. Phys. Lett. **103**, 012602 (2013).
[19] J. M. Chow, J. M. Gambetta, E. Magesan, D. W. Abraham, A. W. Cross, B. R. Johnson, N. A. Masluk, C. A. Ryan, J. A. Smolin, S. J. Srinivasan, and M. Steffen, Implementing a strand of a scalable fault-tolerant quantum computing fabric, Nat. Commun. **5**, 4015 (2014).
[20] Y. Chen, C. Neill, P. Roushan, N. Leung, M. Fang, R. Barends, J. Kelly, B. Campbell, Z. Chen, B. Chiaro, A. Dunsworth, E. Jeffrey, A. Megrant, J. Y. Mutus, P. J. J. O'Malley, C. M. Quintana, D. Sank, A. Vainsencher, J. Wenner, T. C. White, M. R. Geller, A. N. Cleland, and J. M. Martinis, Qubit Architecture with High Coherence and Fast Tunable Coupling, Phys. Rev. Lett. **113**, 220502 (2014).
[21] M. Stern, G. Catelani, Y. Kubo, C. Grezes, A. Bienfait, D. Vion, D. Esteve, and P. Bertet, Flux Qubits with Long Coherence Times for Hybrid Quantum Circuits, Phys. Rev. Lett. **113**, 123601 (2014).
[22] S. Neil, K. Julia, and W. K. Birgitta, Quantum random-walk search algorithm, Phys. Rev. A **67**, 052307 (2003).
[23] C. Di Franco, M. Mc Gettrick, and Th. Busch, Mimicking the Probability Distribution of a Two-Dimensional Grover Walk with a Single-Qubit Coin, Phys. Rev. Lett. **106**, 080502 (2011).

[24] Y. C. Jeong, C. Di Franco, H. T. Lim, M. S. Kim, and Y. H. Kim, Experimental realization of a delayed-choice quantum walk, Nat. Commun. **4**, 2471 (2013).
[25] A. Crespi, R. Osellame, R. Ramponi, V. Giovannetti, R. Fazio, L. Sansoni, F. De Nicola, F. Sciarrino, and P. Mataloni, Anderson localization of entangled photons in an integrated quantum walk, Nat. Photon. **7**, 322 (2013).
[26] X. Zhan, L. Xiao, Z. H. Bian, K. K. Wang, X. Z. Qiu, B. C. Sanders, W. Yi, and P. Xue, Detecting Topological Invariants in Nonunitary Discrete-Time Quantum Walks, Phys. Rev. Lett. **119**, 130501 (2017).
[27] A. Peruzzo, M. Lobino, J. C. F. Mathews, N. Matsuda, A. Politi, K. Poulios, X. Q. Zhou, Y. Lahini, N. Ismail, K. Worhoff, Y. Bromberg, Y. Silberberg, M. G. Thompson, and J. L. O'Brien, Quantum walks of correlated photons, Science **329**, 1500 (2010).
[28] T. Kitagawa, M. S. Rudner, E. Berg, and E. Demler, Exploring topological phases with quantum walk, Phys. Rev. A **82**, 033429 (2010).
[29] A. M. Childs, Universal Computation by Quantum Walk, Phys. Rev. Lett. **102**, 180501 (2009).
[30] M. S. Underwood, and D. L. Feder, Universal quantum computation by discontinuous quantum walk, Phys. Rev. A **82**, 042304 (2010).
[31] A. M. Childs, D. Gosset, and Z. Webb, Universal computation by multiparticle quantum walk, Science **339**, 791 (2013).
[32] P. Kurzynski, and A. Wojcik, Quantum Walk as a Generalized Measuring Device, Phys. Rev. Lett. **110**, 200404 (2013).
[33] P. Rebentrost, M. Mohseni, I. Kassal, S. Lloyd, and A. A. Guzik, Environment-assisted quantum transport, New J. Phys. **11**, 033003 (2009).
[34] M. Montero, Unidirectional quantum walks: Evolution and exit times, Phys. Rev. A **88**, 012333 (2013).
[35] L. Innocenti, H. Majury, T. Giordani, N. Spagnolo, F. Sciarrino, M. Paternostro, and A. Ferraro, Quantum state engineering using one-dimensional discrete-time quantum walks, Phys. Rev. A **96**, 062326 (2017).
[36] L. Sansoni, F. Sciarrino, G. Vallone, P. Mataloni, A. Crespi, R. Ramponi, and R. Osellame, Two-Particle Bosonic-Fermionic Quantum Walk via Integrated Photonics, Phys. Rev. Lett. **108**, 010502 (2012).
[37] P. Xue, R. Zhang, H. Qin, X. Zhan, Z. H. Bian, J. Li, and B. C. Sanders, Experimental Quantum-Walk Revival with a Time-Dependent Coin, Phys. Rev. Lett. **114**, 140502 (2015).
[38] B. Do, M. L. Stohler, S. Balasubramanian, D. S. Elliott, C. Eash, E. Fischbach, M. A. Fischbach, A. Mills, and B. Zwickl, Experimental realization of a quantum quincunx by use of linear optical elements, Opt. Soc. Am. B **22**, 499 (2005).
[39] H. Schimitz, R. Matjeschk, C. Schneider, J. Glueckert, M. Enderlein, T. Huber, and T. Schaetz, Quantum Walk of a Trapped Ion in Phase Space, Phys. Rev. Lett. **103**, 090504 (2009).
[40] F. Zaehringer, G. Kirchmair, R. Gerritsma, E. Solano, R. Blatt, and C. F. Roos, Realization of a Quantum Walk with One and Two Trapped Ions, Phys. Rev. Lett. **104**, 100503 (2010).
[41] M. Karski, L. Forster, J. M. Choi, A. Steffen, W. Alt, D. Meschede, and A. Widera, Quantum walk in position space with single optically trapped atoms, Science **325**, 174 (2009).
[42] P. Xue, B. C. Sanders, A. Blais, and K. Lalumiere, Quantum walks on circles in phase space via superconducting circuit quantum electrodynamics, Phys. Rev. A **78**, 042334 (2008).
[43] A. C. Hardal, P. Xue, Y. Shikano, O. E. Müstecaplioglu, and B. C. Sanders, Discrete time quantum walk with nitrogen-vacancy centers in diamond coupled to a superconducting flux qubit, Phys. Rev. A **88**, 022303 (2013).
[44] E. Flurin, V. V. Ramasesh, S. Hacohen-Gourgy, L. S. Martin, N. Y. Yao, and I. Siddiqi, Observing Topological Invariants Using Quantum Walks in Superconducting Circuits, Phys. Rev. X **7**, 031023 (2017).
[45] J. Ghosh, Simulating Anderson localization via a quantum walk on a one-dimensional lattice of superconducting qubits, Phys. Rev. A **89**, 022309 (2014).
[46] Y. Hirayama, A. Miranowicz, T. Ota, G. Yusa, K. Muraki, S. K. Özdemir, and N. Imoto, Nanometre-scale nuclear-spin device for quantum information processing, J. Phys.: Condens. Matter **18**, S885 (2006).
[47] A. Miranowicz, S. K. Ozdemir, J. Bajer, G. Yusa, N. Imoto, Y. Hirayama, and F. Nori, Quantum state tomography of large nuclear spins in a semiconductor quantum well: Robustness against errors as quantified by condition numbers, Phys. Rev. B **92**, 075312 (2015).
[48] J. Ghosh, Emulating quantum state transfer through a spin-1 chain on a one-dimensional lattice of superconducting qutrits, Phys. Rev. A **90**, 062318 (2014).
[49] T. Liu, S. J. Xiong, X. Z. Cao, Q. P. Su, and C. P. Yang, Efficient transfer of an arbitrary qutrit state in circuit quantum electrodynamics, Opt. Lett. **40**, 5602 (2015).
[50] F. Wang, L. Yu, Q. P. Su, and C. P. Yang, Simple scheme for information transfer of a qutrit in circuit QED, Prog. Theor. Exp. Phys. **2017**, 073J01 (2017).
[51] W. Chen, D. A. Bennett, V. Patel, and J. E. Lukens, Substrate and process dependent losses in superconducting thin film resonators, Supercond. Sci. Technol. **21**, 075013 (2008).
[52] P. J. Leek, M. Baur, J. M. Fink, R. Bianchetti, L. Steffen, S. Filipp, and A. Wallraff, Cavity Quantum Electrodynamics with Separate Photon Storage and Qubit Readout Modes, Phys. Rev. Lett. **104**, 100504 (2010).
[53] F. Yan, S. Gustavsson, A. Kamal, J. Birenbaum, A. P. Sears, D. Hover, T. J. Gudmundsen, D. Rosenberg, G. Samach, S. Weber, J. L. Yoder, T. P. Orlando, J. Clarke, A. J. Kerman, and W. D. Oliver, The flux qubit revisited to enhance coherence and reproducibility, Nat. Commun. **7**, 12964 (2016).
[54] J. Q. You, X. D. Hu, S. Ashhab, and F. Nori, Low-decoherence flux qubit, Phys. Rev. B **75**, 140515(R) (2007).
[55] C. Rigetti, J. M. Gambetta, S. Poletto, B. L. T. Plourde, J. M. Chow, A. D. Corcoles, J. A. Smolin, S. T. Merkel, J. R. Rozen, G. A. Keefe, M. B. Rothwell, M. B. Ketchen, and M. Steffen, Superconducting qubit in a waveguide cavity with a coherence time approaching 0.1 ms, Phys. Rev. B **86**, 100506(R) (2012).
[56] I. M. Pop, K. Geerlings, G. Catelani, R. J. Schoelkopf, L. I. Glazman, and M. H. Devoret, Coherent suppression of electromagnetic dissipation due to superconducting quasiparticles, Nature (London) **508**, 369 (2014).
[57] M. Baur, S. Filipp, R. Bianchetti, J. M. Fink, M. Goppl, L. Steffen, P. J. Leek, A. Blais, and A. Wallraff, Measurement of Autler-Townes and Mollow Transitions in a Strongly Driven Superconducting Qubit, Phys. Rev. Lett. **102**, 243602 (2009).